Nanomed. J. 5(2): 111-120, Spring 2018

RESEARCH PAPER

Enhancement of radio-sensitivity of colorectal cancer cells by gold nanoparticles at 18 MV energy

Mansour Zabihzadeh [1,2], Mojtaba Hoseini-Ghahfarokhi [1,3,4*], Vahid Bayati [5,6], Ali Teimoori [7,8], Zahra Ramezani [3,9], Mohamad-Ali Assarehzadehgan [10], Morteza Pishghadam [11]

[1]Department of Medical Physics, Faculty of Medicine, Ahvaz Jundishapur University of Medical Sciences, Ahvaz, Iran
[2] Department of Clinical Oncology, Golestan Hospital, Ahvaz Jundishapur University of Medical Sciences, Ahvaz, Iran
[3] Nanotechnology Research Center, Faculty of Pharmacy, Ahvaz Jundishapur University of Medical Sciences, Ahvaz, Iran
[4] Student Research Committee, Ahvaz Jundishapur University of Medical Sciences, Ahvaz, Iran
[5] Cellular and Molecular Research Center, Ahvaz Jundishapur University of Medical Sciences, Ahvaz, Iran
[6] Department of Anatomical Sciences, School of Medicine, Ahvaz Jundishapur University of Medical Sciences, Ahvaz, Iran
[7] Health Research Institute, Infectious and Tropical Diseases Research Center, Ahvaz Jundishapur University of Medical Sciences, Ahvaz, Iran
[8] Virology Department, School of Medicine, Ahvaz Jundishapur University of Medical Sciences, Ahvaz, Iran
[9] Department of Medicinal Chemistry, Faculty of Pharmacy, Ahvaz Jundishapur University of Medical Sciences, Ahvaz, Iran
[10] Department of Immunology, Iran University of Medical Sciences, Tehran, Iran
[11] Faculty of Medicine, North Khorasan University of Medical Sciences, Bojnurd, Iran

ABSTRACT

Objective(s): Taking advantage of high atomic number of gold nanoparticles (GNPs) in radiation dose absorbing, many in vitro and in vivo studies have been carried out on using them as radio-sensitizer. In spite of noticeable dose enhancement by GNPs at keV energies, using this energy range for radiotherapy of deep-seated tumors is outdated. The aim of the present work was to examine the effect of GNPs on radio-sensitivity of HT-29 cells in combination with 18 MV X-rays.

Materials and Methods: GNPs were synthesized using a seed-growth method and characterized by transmission electron microscopy (TEM) for size and morphology. Cytotoxicity effect of the GNPs as well as amount of uptake into the HT-29 cell line was assessed. Irradiation was done by 18 MV photons. Immuno-fluorescent imaging of γ-H2AX foci and clonogenic assay were conducted to find out the effect of the GNPs on radio-sensitivity of the cells.

Results: The size of GNPs was about 24 nm with a spherical-like shape. Treatment of the cells with the GNPs induced insignificant inhibition in cell growth. Cellular uptake reaches a maximum after 12 h incubation with GNPs. Stained γ-H2AX foci showed a significant difference in number and intensity for GNPs treated cells compared to only irradiated one. Moreover, colony formation assay proved an impressive decrease in the number of colonies for the irradiated+GNPs group rather than the other one. By fitting the survival fraction data on the linear-quadratic model, sensitization enhancement factor (SER) of 1.25 was achieved.

Conclusion: Although theoretical studies predicted negligible radio-enhancement factor for GNPs at high megavoltage energies, present results show the potential of GNPs for possible gold nanoparticle-aided radiation therapy (GNRT) even for high MV photons.

Keywords: *Colon cancer, Gamma-H2AX, Gold nanoparticles, Megavoltage X-ray, Radiosensitizer*

How to cite this article
Zabihzadeh M, Hoseini-Ghahfarokhi M, Bayati V, Teimoori A, Ramezani Z, Assarehzadehgan MA, Pishghadam M. Enhancement of radio-sensitivity of colorectal cancer cells by gold nanoparticles at 18 MV energy. Nanomed J. 2018; 5(2): 111-120. DOI: 10.22038/nmj.2018.005.008

* *Corresponding Author Email: Hoseini.m@ajums.ac.ir*
Note. This manuscript was submitted on January 2, 2017; approved on February 29, 2018

INTRODUCTION

Radiation therapy as a key modality in cancer cure, has attempted to improve therapeutic gain by delivering dose as much as possible to the tumor site while making it minimum in peripheral normal tissues. However, this issue has remained as a challenge in the field due to the high similarity of both tissues faced with radiation exposure[1]. In this regard, there are two general solutions to compensate the lack of distinction in radiation dose absorbing of healthy and tumorous tissues: loading radio-sensitizers in cancer cells or radio-protector into the normal cells.

Owing to high dependency of photon cross section on atomic number, high Z elements (HZEs) like gold, gadolinium and iodine are the appropriate candidates to be utilized as radio-sensitizers in radiotherapy [2-7]. For photoelectric and pair production process as two important photon interactions with matter in the energy ranges of keV to MeV, the mass attenuation coefficient is proportional to Z^3 and Z, respectively[8]. This brings about a significant increase (more than 100 times) in energy absorption of gold (Z=79) compared to soft tissue (Z=7.6) in keV energy range[9]. Following a photoelectric interaction, the total energy of photon is transferred to an electron which can be ejected and a vacancy will be created. By filling the vacancy with outer shells electrons, a fluorescent photon can be emitted whose energy is sufficient to eject an outer located electron, called Auger electron[8]. This Auger electron with a range of few μm has a key role in the deposition of energy particularly in the vicinity of HZEs used as radio-sensitizers. Thus accumulation of the HZEs into the tumor can lead to the generation of Auger electron and deposition of more dose in the cancerous tissue.

Apart from the suitable physical properties of gold as a contrast agent, low cytotoxicity, high biocompatibility, ease in chemical synthesis and simplicity in surface modification by biological structures like antibodies and aptamers, it has motivated many researchers to study the effect of gold nanoparticles (GNPs) on dose enhancement[10-17].

In a pioneering study carried out by Hainfeld *et al.* [18], it was demonstrated that intravenously injected 1.9 nm GNPs in combination with 250 kVp photons can significantly improve survival of EMT-6 mammary tumors bearing mice. The GNP size effect on radio-sensitization was investigated in vitro on HeLa cell line[19]. As a result, particles with 50 nm in size showed higher dose enhancement factor (DEF) than other sizes which was associated with high intracellular uptake of GNPs with the size and so more occurrence of photoelectric interaction. To implement a targeting strategy, HER2 conjugated GNPs were prepared to elevate formation of γ-H2AX foci in MDA-MB-361 breast cancer cells by about 2-fold compared to bare GNPs[20].

Moreover, tumor size of the HER2-GNP treated mice was reduced by 46% of initial size while the group with radiation alone had an increase in size about 16%. Due to the high metabolic rate of cancer cells, glucose coating could be a good solution to increase accumulation of GNPs into the cells and consequently their radio-sensitization. Some in vitro studies have reported DEFs of 1.24-1.86 utilizing glucose capped GNPs for various types of cancer cell lines such as ovarian carcinoma[21], prostate [22] and cervical [23] cancers, lung carcinoma [24] and breast adenocarcinoma[25]. Recently, a combination of GNPs and Cisplatin as radio-enhancers with 225 kVp x-ray irradiation resulted in a DEF about 1.39 for MDA-MB-231 cell line and also a significant delay in tumor growth of animal model[26].

Exploiting the high absorption coefficient of gold in kV energies to raise production of Auger and photo-electrons has persuaded many researchers to use x-ray sources in the energy range to increase the influence of GNPs in dose enhancement.

Nevertheless, high MV radiation sources are clinically preferential for radiotherapy of deep-seated tumors like colon and prostate due to more penetration depth and sparing of shallow organs. Although some theoretical and simulation works predicted insignificant dose enhancement by a combination of HZEs with MV radiation[2, 6, 27-29], in vitro experiments have had promising results[19, 21, 24, 25, 30-33]. Therefore, it seems there are extra impressive biological factors altering sensitization of cells to radiation which have not been taken into account by physical calculation methods.

The present work aims to investigate radio-sensitization of HT-29 colorectal cancer cell line irradiated by 18 MV photon beam in the presence of GNPs. To our knowledge, this is the first report about using GNP as radio-sensitizer in combination with 18 MV photons in vitro.

MATERIALS AND METHODS

Chemicals

Gold (III) chloride trihydrate (ACS reagent, ≥49.0%), trisodium citrate (99%), bovine serum albumin (BSA), 3-(4,5-Dimethyl-2-thiazolyl)-2,5-diphenyl tetrazolium bromide (MTT), crystal violet and 4',6-Diamidino-2-phenylindole dihydrochloride (DAPI) were purchased from Sigma-Aldrich Chemical Co.(St. Louis, USA).

HPLC grade deionized water, dimethyl sulfoxide (DMSO), HCl and HNO_3 acids, formaldehyde and methanol were obtained from Merck (Darmstadt, Germany) and used in all experiments. All glassware was cleaned with hydrochloric acid (HCl) Merck (Darmstadt, Germany), rinsed with deionized water, and kept at 150 ˚C before use.

GNPs preparation

Synthesis of GNPs was done using a seed-growth method based on the previous report[34]. Briefly, in order to synthesize GNP seeds, 150 mL sodium citrate (2.2 mM) in a two-necked round-bottomed flask equipped with a condenser, was heated on a magnetic hotplate (Heidolph, Germany) under vigorous stirring. Once the solution started to boil, 1 ml of $HAuCl_4$ (25 mM) was immediately added. After about 10 minutes the color of the solution was changed to bluish gray and then pink. The stable color of the solution confirmed seeds production. The process was followed by cooling of the vessel temperature down to 90 ˚C. The temperature ensures that nucleation of new seeds is quenched even in the presence of an extra amount of precursors. To grow GNPs of about 25 nm in size, sodium citrate (1 ml, 60 mM) and $HAuCl_4$ (1 ml, 25 mM) were injected to the seeds solution in a sequential manner. The final product was allowed to reach room temperature and stored in the dark and 4 ˚C until experiment time.

Characterization of prepared GNPs

The size and morphology of the synthesized GNPs were investigated by transmission electron microscopy (TEM). The sample placed on a carbon-coated copper grid was analyzed by a TEM microscope (Zeiss-EM10C, Germany) operating in 100 kV. At least 500 particles were considered to obtain the size histogram. In addition, UV-Visible spectrum of the product was acquired using a spectrophotometer (Nanodrop one^c, Thermo Scientific, USA). The primary concentration of GNPs was determined theoretically by absorbance at 450 nm[35].

Cell culture

Human colon cancer cell line (HT-29) was obtained from Iranian Biological Resource Center (IBRC, Iran). The cells were cultured as monolayer in Dulbecco's modified Eagle's medium (DMEM, Bio-Idea, Iran) containing 4.5 g/dL glucose supplemented by 10% fetal bovine serum (FBS, Gibco, USA) and 1% antibiotic mixture of penicillin/streptomycin (Invitrogen, USA). The culture flasks and plates were maintained at 37 ˚C by an incubator (Memmert, Germany) operating in 5% Co_2 and 90% humidity condition. In all experiments, the cells were in exponential phase of growth. Once the cells confluency was more than 80%, the cells were detached by Trypsin/EDTA (Gibco) and sub-cultured in lower density.

Cytotoxicity of synthesized GNPs

Toxicity effect of GNPs on the cancerous cells was assayed by MTT salt which is reduced by mitochondrial dehydrogenase to formazan. Briefly, the cells were seeded in a flat-bottomed 96-well microplate (SPL Life Sciences, Korea) as 10000 cell per well and incubated in the mentioned condition overnight. Moreover, fresh culture media contained GNPs in final concentrations of 50, 100, 250 and 400 µM were prepared. After overnight incubation, complete media containing different concentrations of GNPs were replaced for each test group. There were three groups in the study: one group as the blank and the other two groups as the control. The cells were allowed to uptake the GNPs for 24 and 48 h in the incubator. Then the medium of each well was discarded, the cells were washed twice by phosphate buffer saline (PBS, Bio-Idea, Iran) and fresh complete medium was added followed by 50 µl MTT solution to all wells. The plates were transferred to the incubator for 4 h under dark condition. Afterwards, the media were aspirated and to dissolve formazan crystals, DMSO was added to each well. The absorbance values of the plate wells were measured using an Elisa reader (BioTek, ELx808, USA) at 570 nm wavelength. The average OD (570) of the blank group was subtracted from all ODs. The viability rate of each group was defined as:

$$\text{Viability rate} = \frac{\text{average OD(570) of the treated group}}{\text{average OD(570) of the control group}} \times 100$$

Quantification of intracellular uptake of GNPs

To determine the amount of the internalized gold to the cells after incubation with GNPs, they were analyzed by atomic absorption spectroscopy (AAS) technique. In short, about 1×10^6 cells were seeded in a 6 well culture plate (SPL Life Sciences, Korea) and incubated overnight. Therefore, the medium was replaced by FBS-free medium containing GNPs in a final concentration of 250 µM. After 12 and 24 h of incubation, free GNPs were removed by aspiration of the medium and washing the cells by PBS twice. The cells were detached by Tryp-EDTA, counted by a hemocytometer and collected by centrifugation. The pellet lysis process was done by adding 10 ml of warmed aqua regia (3:1(v/v) HCl/HNO_3). Then the total mass of the gold was determined by a graphite furnace AAS (Varian 220z, USA). The amount of GNPs uptake in each cell was calculated by the following equation:

$$\text{GNPs per cell}=\frac{\text{measured gold in a pellet}}{\text{total number of the cells in a well}}$$

Irradiation setup

The cells were irradiated by a PRIMUS linear accelerator (Siemens, Germany) installed at Ahvaz Golestan Hospital with 18 MV photon mode. The plates or flasks were immersed in a water phantom and located in the depth of maximum dose (about 3.5 cm). The source to surface distance (SSD) was 100 cm and the unit dose rate was 200 cGy/min. Moreover, the radiation field was opened so that it covered the whole area of cell containers as well considered the penumbra effect.

Visualization of γ-H2AX foci

Since phosphorylated H2AX foci are known as double strand breaks (DSBs) biomarkers[36, 37], to investigate the effect of GNPs on radio-sensitivity of HT-29 cells, the foci are indirectly stained and illustrated by immuno-fluorescent imaging. Shortly, after seeding the cells in two 12 well plate, the wells were classified into three groups as control, irradiation only and GNPs+irradiation. The medium of the latter two groups was changed to GNP containing media and allowed to uptake the GNPs for 12 h. Therefore, the medium of all wells was aspirated and replaced with fresh one. The cells received 8 Gy radiation dose as described before. After 24 h of irradiation, the cells were rinsed with PBS and fixed by adding 4% formaldehyde. Next, permeabilized cells using cold 90% methanol were washed with PBS/BSA. The cells were incubated with diluted (1:400) γ-H2AX primary antibody (Cell Signaling, USA) for 1 h, rinsed 3 times with PBS/BSA and followed by staining with Alexa-Fluor 488 conjugated secondary antibody (diluted 1:500). Moreover, to label DNA content of the cells, they were treated with DAPI. Finally, immuno-fluorescent imaging was carried out using an inverted microscope (OPTIKA, IM-3FL4, Italy). The images were overlaid using ImageJ (V1.51) software.

Colony formation assay

As a gold standard method in radio-biological studies, clonogenic assay was utilized to survey the colony formation potency of HT-29 cells in the presence of GNPs. Considering the groups as described before, T-12 cell culture flasks (Jet Biofil, China) were seeded, treated with/without GNPs and irradiated for 2, 4, 6 and 8 Gy. Immediately after irradiation, the cells were harvested and counted by a hemocytometer. A sufficient number of the cells were seeded in the 6 well plates in triplicate and transferred to the incubator at 37 ˚C for 12 days. Therefore, the cells were fixed in 4% formaldehyde followed by staining the colonies with crystal violet (0.5% w/v). By calculating plating efficiency (PE) for the control group, the survival fractions (SFs) were achieved by the formula:

$$\text{Survival fraction}=\frac{\text{number of colonies}}{\text{number of seeded cells}\times\text{PE}}$$

The response curves of the groups to the radiation were obtained by fitting the data to linear-quadratic model expressed as $S=\exp(-\alpha D-\beta D^2)$. To quantify the impact of GNPs on absorbed dose, sensitization enhancement factor (SER) was also calculated by dividing mean inactivation dose (MID) of the irradiated alone group by GNP treated group.

Statistical Analysis

All experiments were carried out in triplicate. The amount of internalized GNPs and survival data were noted as mean ± standard deviation and the statistical comparison of groups was done by one-way analysis of variance (ANOVA) with the threshold of significance $P<0.05$.

RESULTS AND DISCUSSION

Characterization of GNPs

The synthesis of GNPs was done by seeding growth method. TEM images showed a spherical morphology, and analyzing the images on over 500 particles indicated a mean diameter of 24.7±3.6 nm (Fig .1).

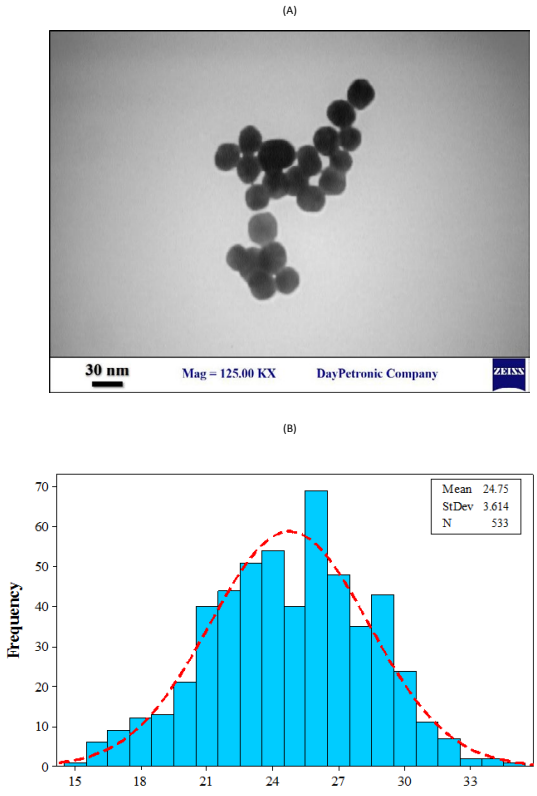

Fig 1. TEM image of synthesized GNPs (A) and size distribution of the nanoparticles (B)

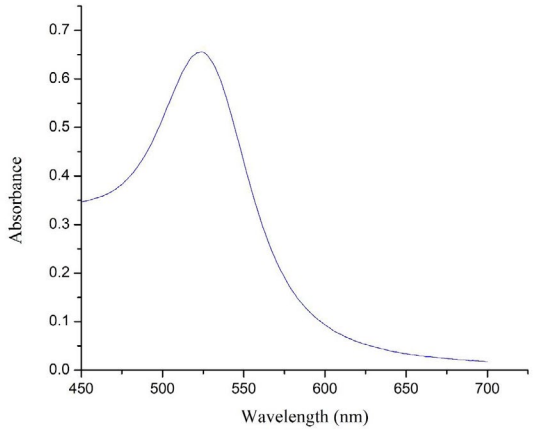

Fig 2. UV-Vis spectrum of the citrate capped GNPs with an absorbance peak at 525 nm

Furthermore, maximum absorbance at 525 nm in the UV-Visible spectrum of the GNPs also confirmed the average size (Fig .2). As expected, the mean size was approximately the same as reported by Bastus *et al.* [34]. In comparison with conventional Turkevich method, the synthesis method has some advantages such as higher monodispersity and concentration.

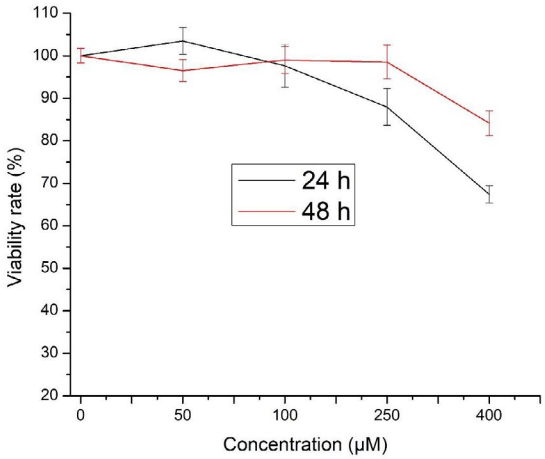

Fig 3. The viability rate of HT-29 cells as a function of GNPs concentration for 24 and 48 h incubation time

Biocompatibility potential of the GNPs

The toxicity effect of the GNPs on the HT-29 cells was evaluated by MTT assay. The reading of all groups was normalized to the control group. As it can be seen in Fig .3, the viability rate is dependent on the concentration of the GNPs. A higher concentration induces more inhibition in cell proliferation which is in agreement with many studies about GNP cytotoxicity [14, 24, 25, 38, 39]. The concentration of 400 μM shows the highest inhibition rate for both incubation time, and after concentration 250 μM, the viability rate suddenly declined with an increase in concentration. It seems for 250 and 400 μM groups, the survival rate recovered from 87.96 and 67.38% for 24 h to 98.53 and 84.16% for 48 h, respectively. This trend was also reported by Zhang *et al.* [39].

Additionally, analyzing the data revealed half maximal inhibitory concentration (IC_{50}) of 526.73 and 756.75 for 24 and 48 incubation time of the GNPs, respectively.

Although the concentration of 400 μM has a significant toxicity effect on the cells, the rest has an acceptable biocompatibility on the treated cells ($P > 0.05$). Chen *et al.* proved that 28 nm Bovine serum albumin (BSA) capped GNPs (0.05 mg/ml) can cause an inhibition rate of about 10% on U87 glioblastoma cell line which is close to our findings[40]. Moreover, it has been shown that the 27.3 nm PEG-GNPs can reduce the growth rate of HeLa cells down to 60% at concentration of 0.25 mM[39]. In their study, the viability rate of the cells in all concentrations was lower than ours. In another study, Rahman *et al* obtained a survival

rate of about 84% for BAEC cells using 0.25 mM 1.9 nm GNPs.

It is well known that in addition to concentration other key factors like size, shape, surface modification and cell type can significantly affect GNPs cytotoxicity. The size effect is well documented in the literature where some researchers have concluded GNPs smaller than 10 nm lead to higher toxicity [38, 39, 41, 42].

It is worth to note that because of the variety in concentration unit notation in the reports (nM, µM, # particles/ml, mg/ml, etc.), it is difficult to compare studies together in detail.

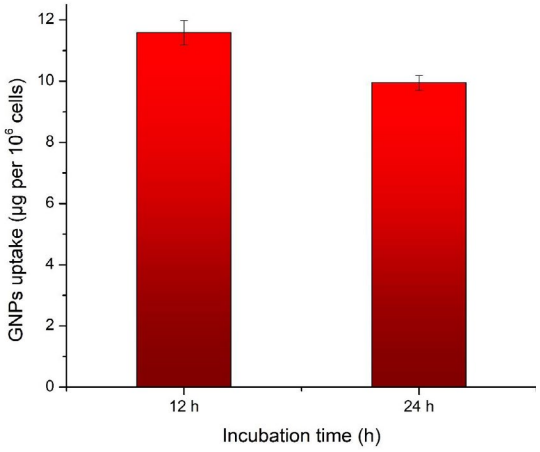

Fig 4. Gold content measured by graphite furnace AAS. The cells are allowed to uptake GNPs for 12 and 24 h incubation time

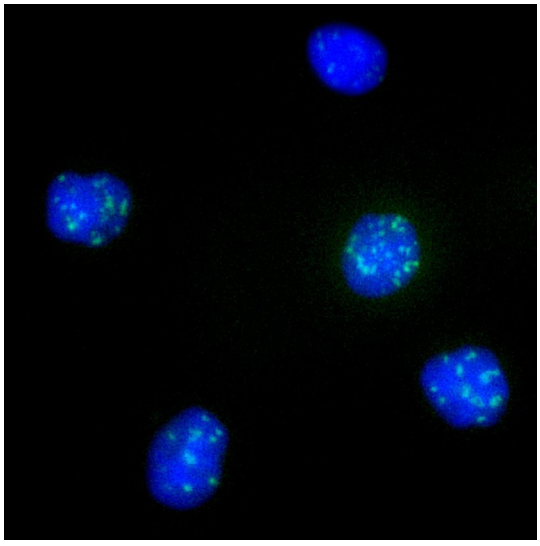

Fig 5. Immuno-fluorescent image of indirect staining of γ-H2AX foci accumulated into the DNA content of HT-29 cells after 8 Gy irradiation by 18 MV photon beam

Uptake GNPs in the cells

The amount of intracellular uptake of the gold was measured by graphite furnace AAS method. It is clear from Fig .4 that the GNPs have significantly penetrated into the cells during both incubation time ($P<0.05$). Furthermore, the gold content of 12 h group is greater than that of 24 h ($P<0.05$). In a separated experiment, we found that among incubation time periods, 48 h group owns the lowest uptake of the GNPs into the cell. Therefore, it appears that uptake has a time-dependent pattern and it culminates after 12 h of incubation for HT-29 cells. Consist with our results, the pattern was also observed in other studies. Wang *et al.* [25], for example, found that the MDA-MB-231 breast cancer cells uptake of 16 and 49 nm GNPs alters by the incubation time with a peak at 24 h. In addition, A549 cells also showed an uptake peak after 24 h followed by a decrease for the 48 h group[24]. However, in the study of Khoshgard *et al.* study [14], uptake pattern versus time exhibited an increasing trend without any peak up to 48 h. It has been uncovered that folic acid-GNPs uptake into the human epidermal KB cells is saturated only 1 hour after incubation[43].

The difference in the uptake pattern could be associated with the GNP size, surface chemistry, charge and type of the cells. In the range of 10-100 nm, 50 nm GNPs showed a maximum rate uptake whose main mechanism of entry into the cells is receptor-mediated endocytosis (RME)[44]. In this respect, Geo *et al.* predicted an optimal size of 27-30 nm for fast RME. Additionally, 20 nm GNPs have been preferred among the other sizes due to their bio-distribution pattern [45].

Surface modification of GNPs as another key factor has extensively been extensively investigated by many researchers to enhance cellular uptake of GNPs. Owing to overexpression of some receptors on the surface of cancerous cells, the receptors were proposed as valuable targets to elevate the availability of the GNPs around the cells [20, 22, 24, 45, 46].

Immuno-fluorescent imaging of γ-H2AX foci

It is well established that DSBs as one of the leading types of the DNA lesion can mainly cause lethal damages after exposure to ionizing radiation [47]. Following the occurrence of DSBs, H2AXs are phosphorylated for serine 139 in their histone and form γ-H2AXs which are concentrated on the DSBs site[48]. Thus, the maker was chosen to investigate

the extent of DNA damage produced by radiation in the presence of GNPs.

The γ-H2AX foci (green) covering damaged DNA of the nucleus (blue color) of 8 Gy irradiated HT-29 cells were represented in Fig .5. In addition, to compare 3 groups of non-irradiated, irradiated only and irradiated+GNP in terms of DSB incidence, images of the cells are collected in Fig .6 for bright field and fluorescent modes with blue and green filters.

Although some foci are detected in the irradiation only group, it is obvious the number of foci as well their intensity in the irradiation+GNP group is meaningfully greater than two other groups. Consequently, it demonstrates the formation of more DSBs in the group due to the presence of GNPs. Besides, the merged images have made a better understanding of the location of foci in each cell (Fig .6).

In a recent study, Chen *et al.* [40] proved that BSA-GNPs increase density of γ-H2AX foci about 2-fold in the irradiated U87 cell line. Also, HER2 conjugated GNPs were responsible for the significant elevation of DSBs formation for MDA-MB-361 cells irradiated by 100 kVp X-rays[20]. In other investigations on HeLa cells[19, 49], this raising in DSB formation due to treatment with GNPs was also observed.

The studies are in concord with our results. Nevertheless, one study reported that there is no significant difference between GNPs treated and untreated groups in the formation of DSBs[30].

Colony formation assay

In order to investigate the effect of GNPs on the radiation sensitivity of HT-29 cells, they were tested for their ability of colony formation after irradiation. Each sample was seeded to a well and allowed to form colonies for 12 days. Afterward, the counted colonies were normalized to the control group. The response of the cells as a function of deposited radiation dose was presented in Fig .7 for two groups of irradiation alone and irradiation+GNP. The statistical coefficients of determination (R^2) of fitted curves for the groups were 0.999 and 0.998, respectively.

As can be seen in the figure, there is a significant decrease in SF of GNP treated group for all doses compared to irradiated alone one ($P<0.05$), with the exception for 2 Gy dose ($P>0.05$). In other words, for achieve a given radiobiological endpoint, a lower dose is required for GNP treated samples. Similarly, the result of the previous section also predicted this manner. There is evidence about the correlation between observed residual γ-H2AX foci and survival fraction of irradiated cells[50].

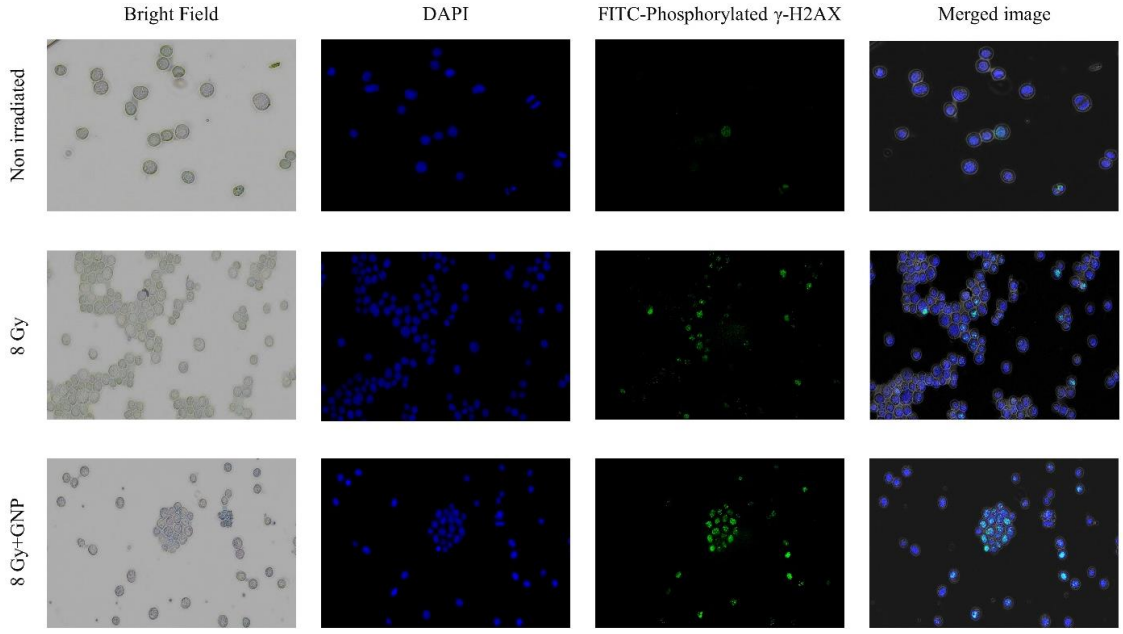

Fig 6. Columns: images of bright field and indirect immune-staining of HT-29 cells for DAPI (blue), FITC γ-H2AX (green) and merged of them. Rows: images of 3 groups of control (non-irradiated), only irradiated (8 Gy) and irradiation+GNPs

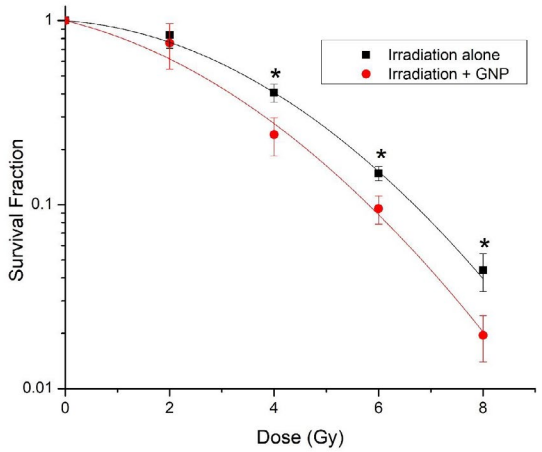

Fig 7. The graph of clonogenic survival assay for HT-29 cells after exposure of 8 Gy 18 MV photon. Fitted curves based on the linear-quadratic model for both groups of irradiation alone (red) and irradiation+GNP (black) were presented. * P<0.05

Furthermore, the decrease has a dose-dependent manner where the proportion of SFs in a given dose raises from 1.1 to 2.25 for 2-8 Gy doses. This could be attributed to the production of further secondary electrons in higher doses.

Likewise, some radiobiological parameters like α, β, $D_{10\%}$ (a dose that is enough to kill 90% of irradiated cells) were extracted from the linear-quadratic model fitted curves (Table .1). According to this table, the linear coefficient (α) of the model has markedly increased for GNP exposed group while it slightly decreased in the quadratic one (β). Moreover, by comparing $D_{10\%}$ of two groups, it can be found that to kill 90% of the cells, the irradiated+GNP group needs to about 15% dose lower than that of the only irradiated group. As a key factor, SER was also reported in the table which represented the amount of enhancement in radiation damages by GNPs.

However, owing to lack of a unique quantity to report as well the variety in the calculation of enhancement factor among the related studies, it is difficult to compare them accurately with the study.

Considering studies with GNP sizes similar to this work, Chen *et al.* [40] have reported a DEF of 1.37 for U87 cell line using 27 nm BSA-GNPs and 160 kVp X-ray source. HER2 targeted GNPs showed a radiation enhancement factor of 1.6 in combination with 100 kVp X-rays[20]. Again in the range of keV energy, Glucose coated GNPs caused an enhancement of dose greater than 30%[51]. The differences may originate from the cell type, concentration, energy and surface modification.

In comparison with our results, keV energies show a higher enhancement factor. The occurrence probability of photoelectric process is elevated in the energy range and generates a large number of photo- and Auger electrons which mainly deposit their energy in situ, as discussed previously. At MeV range, the Compton and pair production processes become dominant. They create scattered photons and secondary electrons whose energy is deposited farther than the interaction site.

Despite the prediction of theoretical and simulation studies about the minor impact on GNPs in megavoltage energies, there is some experimental evidence which have reported promising results. For instance, 6 MV photon beam demonstrates an enhancement of radiation sensitivity of 1.17, 1.3, 1.29 and 1.49 for HeLa [19], SK-OV-3 [21], MDA-MB-231 [30] and A549 [24] cell lines, respectively. Interestingly, GNP treated DU-145 prostate cancer cells were sensitized at 15 MV photon beam by a factor of 1.16 [30] which is close to our calculated SER. In another study using 18 MV energy, measurement in a phantom revealed only 12% dose enhancement even for high GNP concentration of 5 mg/ml [52]. Nonetheless, our results have a significant disagreement with calculated DEF (1.25 vs 1.005 [28]). It seems the vacancy must be filled by non-physical reasons.

Table 1. Radiobiological parameters α, β, D10% and SER derived from fitted curves of Irradiation alone and 8 Irradiation+GNP groups

	α (Gy^{-1})	β (Gy^{-2})	$D_{10\%}$	SER
Irradiation alone	0.046± 0.025	0.045±0.004	6.68	1.25
Irradiation+GNP	0.157±0.052	0.041±0.008	5.80	

It is well established that GNPs can regulate cell cycle [22] and produce more reactive oxygen species (ROS) [21] which have crucial roles in radio-sensitization of the cells. The Glu-GNPs arrested the breast cancer cells in G2/M phase of cell cycle, the most sensitive phase of the cell cycle to radiation damage[24]. Therefore, it can be one of the reasons which affect the radio-sensitivity of the cells and need to be examined.

CONCLUSION

In present study, after synthesizing GNPs with a high concentration, the extent of their uptake

into a colorectal cancer cells line (HT-29) as a deep-seated tumor was evaluated. Moreover, the cytotoxicity test unfolded that viability of the cells is not so affected by applying low concentration GNPs. Similar to clinical situations for such deep-seated tumors, 18 MV photon beam was selected for irradiation of the samples. Surprisingly, analysis of the result of γ-H2AX foci imaging as well as colony formation assay for irradiation+GNP groups unveiled that GNPs can be more helpful than the prediction of theoretical and Monte Carlo simulation. In conclusion, according to our results GNPs were found to have a promising future in clinic as a radio-sensitizer of tumors even at high megavoltage energies, but further in vitro and in vivo investigations are needed.

ACKNOWLEDGMENTS

This report was a part of Ph.D. thesis results of the first author. The authors would like to thank all people who technically helped the work. The thesis was financially supported by Vice-Chancellor for Research Affairs of Ahvaz Jundishapur University of Medical Sciences (Grant code: N-101).

Conflict of Interest

There is no conflict of interest.

REFERENCES

1.Butterworth KT, McMahon SJ, Currell FJ, Prise KM. Physical basis and biological mechanisms of gold nanoparticle radiosensitization. Nanoscale. 2012; 4(16): 4830-4838.
2.Robar JL, Riccio SA, Martin M. Tumour dose enhancement using modified megavoltage photon beams and contrast media. Phys Med Biol. 2002; 47(14): 2433-2449.
3.Kobayashi K, Usami N, Porcel E, Lacombe S, Le Sech C. Enhancement of radiation effect by heavy elements. Mutat Res Rev Mutat Res. 2010; 704(1): 123-131.
4.Luchette M, Korideck H, Makrigiorgos M, Tillement O, Berbeco R. Radiation dose enhancement of gadolinium-based AGuIX nanoparticles on HeLa cells. Nanomedicine. 2014; 10(8): 1751-1755.
5.Babaei M, Ganjalikhani M. A systematic review of gold nanoparticles as novel cancer therapeutics. Nanomed J. 2014; 1(4): 211-219.
6.Cho SH. Estimation of tumour dose enhancement due to gold nanoparticles during typical radiation treatments: a preliminary Monte Carlo study. Phys Med Biol. 2005; 50(15): N163-173.
7.Miladi I, Alric C, Dufort S, Mowat P, Dutour A, Mandon C, Laurent G, Bräuer-Krisch E, Herath N, Coll JL. The in vivo radiosensitizing effect of gold nanoparticles based MRI contrast agents. Small. 2014; 10(6): 1116-1124.
8.Khan FM, Gibbons JP. Khan's the physics of radiation therapy: Lippincott Williams & Wilkins; 2014.
9.Hubbell J, Seltzer S. Tables of X-ray mass attenuation coefficients and mass energy-absorption coefficients (version 1.4). NIST, Gaithersburg, MD. 2004.
10.Ferrero V, Visonà G, Dalmasso F, Gobbato A, Cerello P, Strigari L, Visentin S, Attili A. Targeted dose enhancement in radiotherapy for breast cancer using gold nanoparticles, part 1: A radiobiological model study. Med Phys. 2017; 44(5): 1983-1992.
11.McQuaid HN, Muir MF, Taggart LE, McMahon SJ, Coulter JA, Hyland WB, Jain S, Butterworth KT, Schettino G, Prise KM. Imaging and radiation effects of gold nanoparticles in tumour cells. Sci Rep. 2016; 6: 19442.
12.McNamara A, Kam W, Scales N, McMahon S, Bennett J, Byrne H, Schuemann J, Paganetti H, Banati R, Kuncic Z. Dose enhancement effects to the nucleus and mitochondria from gold nanoparticles in the cytosol. Phys Med Biol. 2016; 61(16): 5993-6010.
13.Kim S-R, Kim E-H. Gold nanoparticles as dose-enhancement agent for kilovoltage X-ray therapy of melanoma. Int J Radiat Biol. 2017; 93(5): 517-526.
14.Khoshgard K, Hashemi B, Arbabi A, Rasaee MJ, Soleimani M. Radiosensitization effect of folate-conjugated gold nanoparticles on HeLa cancer cells under orthovoltage superficial radiotherapy techniques. Phys Med Biol. 2014; 59(9): 2249-2263.
15.Mousavi M, Nedaei HA, Khoei S, Eynali S, Khoshgard K, Robatjazi M, Iraji Rad R. Enhancement of radiosensitivity of melanoma cells by pegylated gold nanoparticles under irradiation of megavoltage electrons. Int J Radiat Biol. 2017; 93(2): 214-221.
16.Rezaee Z, Yadollahpour A, Bayati V, Dehbashi FN. Gold nanoparticles and electroporation impose both separate and synergistic radiosensitizing effects in hT-29 tumor cells: an in vitro study. Int J Nanomedicine. 2017; 12: 1431-1439.
17.Arab-Bafrani Z, Saberi A, Tahmasebi Birgani MJ, Shahbazi-Gahrouei D, Abbasian M, Fesharaki M. Gold nanoparticle and mean inactivation dose of human intestinal colon cancer HT-29 cells. JUNDISHAPUR J NAT PHARM PROD. 2015; 10(4).
18.James FH, Daniel NS, Henry MS. The use of gold nanoparticles to enhance radiotherapy in mice. Phys Med Biol. 2004; 49(18): N309-315.
19.Chithrani DB, Jelveh S, Jalali F, van Prooijen M, Allen C, Bristow RG, Hill RP, Jaffray DA. Gold nanoparticles as radiation sensitizers in cancer therapy. Radiat Res. 2010; 173(6): 719-728.
20.Chattopadhyay N, Cai Z, Kwon YL, Lechtman E, Pignol J-P, Reilly RM. Molecularly targeted gold nanoparticles enhance the radiation response of breast cancer cells and tumor xenografts to X-radiation. Breast Cancer Res Treat. 2013; 137(1): 81-91.
21.Geng F, Song K, Xing JZ, Yuan C, Yan S, Yang Q, Chen J, Kong B. Thio-glucose bound gold nanoparticles enhance radio-cytotoxic targeting of ovarian cancer. Nanotechnology. 2011; 22(28): 285101.
22.Roa W, Zhang X, Guo L, Shaw A, Hu X, Xiong Y, Gulavita S, Patel S, Sun X, Chen J. Gold nanoparticle sensitize radiotherapy of prostate cancer cells by regulation of the cell cycle. Nanotechnology. 2009; 20(37): 375101.
23.Kaur H, Pujari G, Semwal MK, Sarma A, Avasthi DK. In vitro studies on radiosensitization effect of glucose capped gold nanoparticles in photon and ion irradiation of HeLa cells. Nucl Instrum Methods Phys Res B. 2013; 301: 7-11.
24.Wang C, Li X, Wang Y, Liu Z, Fu L, Hu L. Enhancement of radiation effect and increase of apoptosis in lung cancer cells

by thio-glucose-bound gold nanoparticles at megavoltage radiation energies. J Nanopart Res. 2013; 15(5): 1642.
25.Wang C, Jiang Y, Li X, Hu L. Thioglucose-bound gold nanoparticles increase the radiosensitivity of a triple-negative breast cancer cell line (MDA-MB-231). Breast Cancer. 2015; 22(4): 413-420.
26.Cui L, Her S, Dunne M, Borst GR, De Souza R, Bristow RG, Jaffray DA, Allen C. Significant Radiation Enhancement Effects by Gold Nanoparticles in Combination with Cisplatin in Triple Negative Breast Cancer Cells and Tumor Xenografts. Radiat Res. 2017; 187(2): 147-160.
27.Mesbahi A, Jamali F. Effect of photon beam energy, gold nanoparticle size and concentration on the dose enhancement in radiation therapy. BioImpacts: BI. 2013 ;3(1): 29-35.
28.Roeske JC, Nuñez L, Hoggarth M, Labay E, Weichselbaum RR. Characterization of the theorectical radiation dose enhancement from nanoparticles. Technol Cancer Res Treat. 2007; 6(5): 395-401.
29.Lechtman E, Chattopadhyay N, Cai Z, Mashouf S, Reilly R, Pignol J. Implications on clinical scenario of gold nanoparticle radiosensitization in regards to photon energy, nanoparticle size, concentration and location. Phys Med Biol. 2011; 56(15): 4631-4647.
30.Jain S, Coulter JA, Hounsell AR, Butterworth KT, McMahon SJ, Hyland WB, Muir MF, Dickson GR, Prise KM, Currell FJ. Cell-specific radiosensitization by gold nanoparticles at megavoltage radiation energies. Int J Radiat Oncol Biol Phys. 2011; 79(2): 531-539.
31.Liu C-J, Wang C-H, Chien C-C, Yang T-Y, Chen S-T, Leng W-H, Lee C-F, Lee K-H, Hwu Y, Lee Y-C. Enhanced x-ray irradiation-induced cancer cell damage by gold nanoparticles treated by a new synthesis method of polyethylene glycol modification. Nanotechnology. 2008; 19(29): 295104.
32.Rahman WN, Bishara N, Ackerly T, He CF, Jackson P, Wong C, Davidson R, Geso M. Enhancement of radiation effects by gold nanoparticles for superficial radiation therapy. Nanomedicine. 2009; 5(2): 136-142.
33.Wolfe T, Chatterjee D, Lee J, Grant JD, Bhattarai S, Tailor R, Goodrich G, Nicolucci P, Krishnan S. Targeted gold nanoparticles enhance sensitization of prostate tumors to megavoltage radiation therapy in vivo. Nanomedicine. 2015; 11(5): 1277-1283.
34.Bastús NG, Comenge J, Puntes V. Kinetically controlled seeded growth synthesis of citrate-stabilized gold nanoparticles of up to 200 nm: size focusing versus Ostwald ripening. Langmuir. 2011; 27(17): 11098-11105.
35.Haiss W, Thanh NT, Aveyard J, Fernig DG. Determination of size and concentration of gold nanoparticles from UV– Vis spectra. Anal Chem. 2007; 79(11): 4215-4221.
36.Kuo LJ, Yang L-X. γ-H2AX-a novel biomarker for DNA double-strand breaks. In Vivo. 2008;22(3):305-309.
37.Kinner A, Wu W, Staudt C, Iliakis G. γ-H2AX in recognition and signaling of DNA double-strand breaks in the context of chromatin. Nucleic Acids Res. 2008; 36(17): 5678-5694.
38.Pan Y, Neuss S, Leifert A, Fischler M, Wen F, Simon U, Schmid G, Brandau W, Jahnen-Dechent W. Size-dependent cytotoxicity of gold nanoparticles. Small. 2007; 3(11): 1941-1949.
39.Zhang X-D, Wu D, Shen X, Chen J, Sun Y-M, Liu P-X, Liang X-J. Size-dependent radiosensitization of PEG-coated gold nanoparticles for cancer radiation therapy. Biomaterials. 2012; 33(27): 6408-6419.
40.Chen N, Yang W, Bao Y, Xu H, Qin S, Tu Y. BSA capped Au nanoparticle as an efficient sensitizer for glioblastoma tumor radiation therapy. RCS Adv. 2015; 5(51): 40514-40520.
41.Tsoli M, Kuhn H, Brandau W, Esche H, Schmid G. Cellular uptake and toxicity of Au55 clusters. Small. 2005; 1(8-9): 841-844.
42.Pan Y, Leifert A, Ruau D, Neuss S, Bornemann J, Schmid G, Brandau W, Simon U, Jahnen-Dechent W. Gold nanoparticles of diameter 1.4 nm trigger necrosis by oxidative stress and mitochondrial damage. Small. 2009; 5(18): 2067-2076.
43.Li X, Zhou H, Yang L, Du G, Pai-Panandiker AS, Huang X, Yan B. Enhancement of cell recognition in vitro by dual-ligand cancer targeting gold nanoparticles. Biomaterials. 2011; 32(10): 2540-2545.
44.Chithrani BD, Ghazani AA, Chan WC. Determining the size and shape dependence of gold nanoparticle uptake into mammalian cells. Nano lett. 2006; 6(4): 662-668.
45.Geng F, Xing JZ, Chen J, Yang R, Hao Y, Song K, Kong B. Pegylated glucose gold nanoparticles for improved in-vivo bio-distribution and enhanced radiotherapy on cervical cancer. J Biomed Nanotechnol. 2014; 10(7): 1205-1216.
46.Kong T, Zeng J, Yang J, Yao Y, Wang X, Li P, Yang A, Roa W, Xing J, Chen J. Surface modifications of gold-nanoparticles to enhance radiation cytotoxicity. 2007 IEEE/NIH Life Science Systems and Applications Workshop, LISA. 2008: 265-268.
47.Bracalente C, Ibañez IL, Molinari B, Palmieri M, Kreiner A, Valda A, Davidson J, Durán H. Induction and Persistence of Large γH2AX Foci by High Linear Energy Transfer Radiation in DNA-Dependent protein kinase–Deficient Cells. Int J Radiat Oncol Biol Phys. 2013; 87(4): 785-794.
48.Monteiro FL, Baptista T, Amado F, Vitorino R, Jerónimo C, Helguero LA. Expression and functionality of histone H2A variants in cancer. Oncotarget. 2014; 5(11): 3428–3443.
49.Ngwa W, Korideck H, Kassis AI, Kumar R, Sridhar S, Makrigiorgos GM, Cormack RA. In vitro radiosensitization by gold nanoparticles during continuous low-dose-rate gamma irradiation with I-125 brachytherapy seeds. Nanomedicine. 2013; 9(1): 25-27.
50.Banáth JP, Olive PL. Expression of phosphorylated histone H2AX as a surrogate of cell killing by drugs that create DNA double-strand breaks. Cancer Res. 2003; 63(15): 4347-4350.
51.Zhang X, Xing JZ, Chen J, Ko L, Amanie J, Gulavita S, Pervez N, Yee D, Moore R, Roa W. Enhanced radiation sensitivity in prostate cancer by gold-nanoparticles. Clinical & Investigative Medicine. 2008; 31(3): 160-167.
52.Mousavie Anijdan S, Shirazi A, Mahdavi S, Ezzati A, Mofid B, Khoei S, Zarrinfard M. Megavoltage dose enhancement of gold nanoparticles for different geometric set-ups: Measurements and Monte Carlo simulation. Iranian Journal of Radiation Research. 2012; 10(3): 183-186.